35th Annual International Conference of the IEEE EMBS
Osaka, Japan, 3 - 7 July, 2013

Application of Fuzzy Skeletonization to Quantitatively Assess Trabecular Bone Micro-Architecture

Dakai Jin, Yinxiao Liu, and Punam K. Saha*, *Senior Member, IEEE*

Abstract—**Adult bone diseases, especially osteoporosis, lead to increased risk of fracture associated with substantial morbidity, mortality, and financial costs. Clinically, osteoporosis is defined by low bone mineral density; however, increasing evidence suggests that the micro-architectural quality of trabecular bone (TB) is an important determinant of bone strength and fracture risk. Skeletonization plays an important role providing a compact representation of TB network that allows computation of several quantitative parameters relating to TB micro-architecture. Literature of three-dimensional skeletonization is quite matured for binary digital objects. However, the challenges of skeletonization for fuzzy objects are mostly unanswered. Here, an algorithm for fuzzy skeletonization is presented using fuzzy grassfire propagation and a branch-level noise pruning strategy and, finally, its application to TB micro-architectural assessment is investigated. Specifically, the fuzzy skeletonization algorithm is applied to compute TB plateness, plate/rod ratio, thickness, and spacing. Finally, the effectiveness of these measures to predict experimental bone strength is investigated on twelve cadaveric specimens and the results are encouraging with the R^2 value of linear correlation with bone strength being as high as 0.93, 0.88, 0.85 and 0.86, respectively.**

I. Introducation

Osteoporosis increases the risk of fractures associated with substantial morbidity, mortality, and financial costs. Approximately, 30% of postmenopausal white women in the United States suffer from osteoporosis and the prevalence in Europe and Asia is similar. Approximately one in two women and one in four men over age 50 will have an osteoporosis-related fracture in their remaining lifetime. Clinically, osteoporosis is defined by low bone mineral density (BMD). However, increasing evidence suggests that micro-architectural quality of trabecular bone (TB) is an important determinant of bone strength and fracture risk [1]. BMD only explains about 65% to 75% of the variance in bone strength [2], while the remaining variance is due to the cumulative and synergistic effect of various factors including bone macro- and micro-architecture, tissue composition, and micro-damage. In this paper, we investigate the application of fuzzy skeletonization to quantitatively assess TB micro-architecture at *in vivo* imaging resolution.

Several 3D skeletonization algorithms [3-7] have been reported for binary digital objects. But the same is not true for fuzzy skeletonization. Although, a few works on gray scale skeletonization have been presented in literature [8,9], the fundamental challenges related to fuzzy skeletonization are mostly unanswered and a complete skeletonization algorithm for fuzzy digital objects is missing. Here, a framework and an algorithm for fuzzy surface skeletonization are developed using a notion of fuzzy grassfire propagation. The process of fuzzy grassfire propagation is simulated using fuzzy distance transform (FDT) [10]. Arcelli and Baja [11] first used DT in skeletonization in 2-D and discussed its advantages. Saito and Torowaki [6] and others [3] have used DT to define the voxel erosion sequence. Here, a fuzzy skeletonization algorithm is presented using a notion of fuzzy grassfire propagation and a skeletal noise pruning strategy is defined using significance measures at individual skeletal branch level. The role of fuzzy skeletonization in computing individual TB plate width and their characterization on the continuum between a perfect plate and a perfect rod is examined. Also, the fuzzy skeletonization algorithm is applied to compute TB thickness and marrow spacing. Finally, the effectiveness of these measures to predict experimental bone strength has been investigated on twelve cadaveric specimens and the results are presented.

II. Fuzzy Skeletonization Algorithm

Blum's pioneering work on grassfire transform [12] led to the notion of skeletonization that converts a volumetric object into a union of surfaces and curves. The process is intuitively defined using fire propagation on a grass field, where the field resembles an object. The fire is simultaneously set at all boundary points of the field and it propagates inwardly at a uniform speed. The skeleton is defined as the set of quench points, i.e., the points where two or more fire fronts meet. However, the notion of skeletonization for fuzzy objects is not well known. To define a fuzzy skeletonization process, we suggest modifying the Blum's grassfire transform for a fuzzy object where the membership function is interpreted as local material density. In this way, the fuzzy grassfire transform is exactly the same as Blum's original process except that the speed of fire at a given point is inversely proportional to its material density. Thus, fuzzy distance transform (FDT) [10], the least amount of material to be traversed to reach to a point p is proportional to the time when the fire front reaches p. Therefore, during the fuzzy grassfire propagation, the speed of a fire front at a point equates to the inverse of local material density and this equality is violated only at quench points where the propagation process is interrupted. Thus, a voxel $p \in Z^3$, where Z is the set of integers and Z^3 represents a rectangular image grid, is a *quench voxel* in a fuzzy digital object $\mathcal{O} = \{(p, f_O(p)) \mid p \in Z^3 \wedge f_O: Z^3 \rightarrow [0,1]\}$ if the following inequality holds for every neighbor q of p

*Resrach supported by NIH R01-AR054439.

D. Jin is with the University of Iowa, Iowa City, IA 52246 USA (e-mail: dakai-jin@uiowa.edu).

Y. Liu is with the University of Iowa, Iowa City, IA 52246 USA (e-mail: yinxiao-liu@uiowa.edu).

P. K. Saha, is with the University of Iowa, Iowa City, IA 52246 USA. (Phone: 319-936-1466; e-mail: punam-saha@uiowa.edu).

$$FDT(q) - FDT(p) < \tfrac{1}{2}\big(f_O(p) + f_O(q)\big)|p - q|, \quad (1)$$

During the process of fuzzy skeletonization, voxels are removed in the increasing order of FDT values. The overall fuzzy skeletonization process for a fuzzy object O is schematically presented in the following. Here, $O = \{p \mid f_O(p) > 0\}$ denotes the support of the fuzzy object O.

Primary skeletonization

select voxels $p \in O$ in the order of FDT values
  if p is not an axial voxel
    if removal of p preserves 3D topology of O
      if removal of p preserves 2D topology on mid-planes
        remove p from O, i.e., set $f_O(p) = 0$

Final skeletonization:

select voxels $p \in O$ in the order of FDT values
  if p belongs to a two-voxel thick structure
    if removal of p preserves 3D topology of O
      if removal of p preserves 2D topology on mid-planes
        remove p from O, i.e., set $f_O(p) = 0$
select voxels $p \in O$ in the order of FDT values
  if topologic and geometric features of p does not match
    if removal of p preserves 3D topology of O
      remove p from O, i.e., set $f_O(p) = 0$

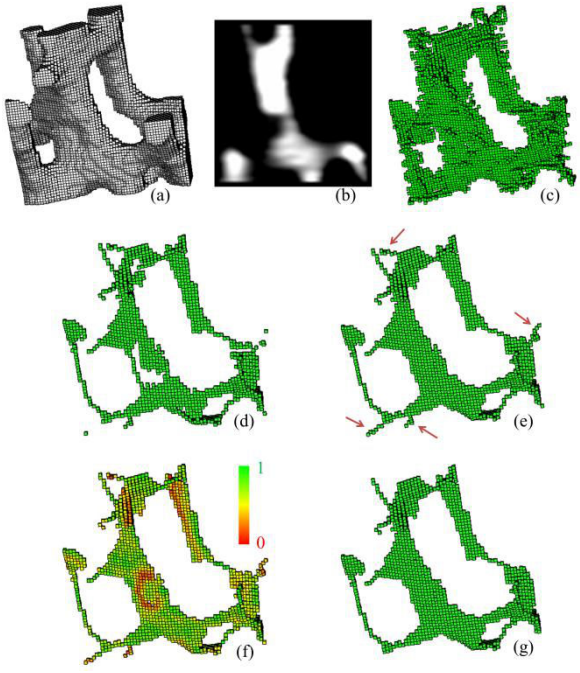

Fig. 1. Results of intermediate steps of fuzzy skeletonization. (a) 3D display of trabecular bone region in a micro-CT image of a cadaveric distal tibia specimen. (b) A sagittal image slice displaying the fuzziness in the image. (c) All quench voxels before filtering with local significance measure. (d) All axial voxels after local significance analyses. (e,f) Results of final skeletonization (e) and local significance computation (f). (g) Final results after noisy branch pruning.

Removal of a voxel $p \in O$ preserves the topology of O if and only if p is a (26,6) simple voxel [13] in O. Beside the 3D topology preservation condition, an additional constrain of 2D topology preservation [14] in all three middle planes of the candidate voxel is subjected to ensure the continuity of surface-like structures and to avoid undesired drilling effects as illustrated by Saha et al. [5]. To complete the description of primary and final skeletonization algorithms, axial voxels, two-voxel thick structures and their removal strategy will be defined. Finally, a pruning algorithm removing noisy skeletal branches will be described.

A. *Axial Voxel*

An axial voxel resembles to a quench voxel of grassfire transform constituting the skeleton of an object. During grassfire transform in a continuous space, two types of quench points are formed: surface- and curve-quench points. In a digital space, surface-quench voxel is formed when two opposite fire fronts meet along x-, y- or z-direction and a curve-quench voxel is formed when fire fronts meet from all directions in xy-, yz-, or zx-planes. A voxel $p = (p_x, p_y, p_z) \in O$ is an *x-surface-quench voxel* if the following two conditions are satisfied by three neighboring voxels $p_{x-} = (p_x - 1, p_y, p_z)$, $p_{x+} = (p_x + 1, p_y, p_z)$, and $p_{x++} = (p_x + 2, p_y, p_z)$:

1) $FDT(p) > FDT(p_{x-})$,

2) $FDT(p) > FDT(p_{x+})$, OR,

$$FDT(p) = FDT(p_{x+}) \wedge FDT(p) > FDT(p_{x++}).$$

To define a curve-quench voxel, let us first consider the formulation of the situation when fire fronts meet in the xy-plane. Curve quench voxels may form a 2x2 clique on the xy-plane. Let $P_{\text{xy}} = \{(p_x, p_y, p_z), (p_x + 1, p_y, p_z), (p_x, p_y + 1, p_z), (p_x + 1, p_y + 1, p_z)\}$ denote the 2x2 clique. Let $Q(P_{\text{xy}})$ denote the set of voxels within the 2x2 clique P_{xy} with their FDT value identical to that of p, i.e.,

$$Q(P_{xy}) = \{q \mid q \in P_{xy} \wedge FDT(q) = FDT(p)\}.$$

Thus, the fire fronts reach simultaneously at every voxel of $Q(P_{\text{xy}})$ from all directions on the xy-plane. Therefore, a voxel $p = (p_x, p_y, p_z) \in O$ is an *xy-curve-quench voxel* if the following condition holds for $\forall\, q \in M_{\text{xy}}(p) - Q(P_{\text{xy}})$

$$q \text{ is 26-adjacent to } Q(P_{\text{xy}}) \;\Rightarrow\; FDT(q) < FDT(p),$$

where, $M_{\text{xy}}(p)$ is the set of all voxels $\{q = (q_x, q_y, q_z) \mid q \in Z^3 \wedge q_x = p_x\}$ constructing the xy-plane through p.

Although the quench voxels captures the notion of fuzzy grassfire transform, it suffers from the fact that a large number of spurious quench voxels are created (Fig. 1(c)). Therefore, it is imperative to filter out some of these quench voxels based on their significance. Here, we introduce a function that resembles the "local significance factor" (LSF) of individual voxels and use LSF measures in the neighborhood to determine the significance of a quench voxel. *Local significance factor* or *LSF* of any voxel $p \in O$, denoted by $LSF(p)$, is defined as follows:

$$LSF(p) = 1 - f_+\left(\max_{q\in N^*(p)} \frac{FDT(q)-FDT(p)}{\frac{1}{2}(f_O(p)+f_O(q))|p-q|}\right), \quad (2)$$

where the function $f_+(x)$ returns the value of the input x if $x > 0$ and zero otherwise. The formulation of the above equation follows the arguments of Equation 1. Note the term inside the function f_+ essentially represents the inverse of speed of fire front propagation at the voxel p normalized by local material density. Significance of a surface or curve quench voxel is determined by analyzing the average LSF value of its neighboring voxels. Specifically, a surface or a curve quench is defined as a significant surface or significant curve quench voxels if the average LSF value in the respective neighborhood is greater than a preset threshold value τ. Finally, any significant surface- or curve-quench voxel is referred to as an *axial voxel*.

B. Final Skeletonization

Grassfire propagation in a digital space often leaves two-voxel thick quench structures after primary skeletonization. The purpose of final skeletonization is to convert two-voxel thick structures into single-voxel thick structures and it is completed in two steps. Intuitively, a voxel is two-voxel thick if its three non-opposite 6-neighbors are skeletal voxels and forms two-voxel thick surface across x-, y-, and/or z-direction [5]. During the first step, voxels are considered for erosion in the order of their FDT values. A voxels satisfying two-voxel thickness along all three coordinate directions is deleted if it is a (26, 6) simple voxel. A voxel satisfying two-voxel thickness along two directions, say x and y, is deleted if it is a (26, 6) simple voxel and it preserves 2D topology in $M_{xy}(p)$. Finally, a voxel satisfying two-voxel thickness along only one directions, say x, is deleted if it is a (26, 6) simple voxel and it preserves 2D topology in both $M_{xy}(p)$ and $M_{zx}(p)$. The purpose of the second step of final skeletonization is to remove voxels with contradicting topological and geometric properties.

C. Skeleton Pruning

The primary goal of a skeleton pruning algorithm is to discriminate between significant and non-significant branches so that only false branches may be removed. This goal is accomplished by computing LSF-weighted length of an individual branch from its edge to the corresponding junction voxel. This LSF-weighted branch length is used as a global significance factor of a specific skeletal branch. This overall process is implemented using the following steps – (1) digital topological analysis (DTA), (2) conversion of two-voxel wide curve-like structures into a true digital curve, (3) computation of global significance factors, and (4) removal of non-significant branches.

III. Experiment Results

Results of intermediate steps of skeletonization and pruning on a small region of trabecular bone image are illustrated in Fig. 1. To examine the role of fuzzy skeletonization to assess TB micro-architectural quality, two methods were implemented using fuzzy skeletonization – (1) volumetric topological analyses [15] and (2) TB thickness and spacing computations [16]. The first method computes individual trabecular plate width and characterization of plateness and plate-to rod ratio using unique algorithms digital topological analyses, manifold distance transform, and feature propagation [15]. This method generates average trabecular plate or surface width (SW_{VTA}) and plate-to-rod or surface-to-curve ratio (SCR_{VTA}) over a region-of-interest (ROI). The second method computes local TB thickness and spacing using star line based minimum intercept computation and feature propagation [16] and it returns average TB thickness (TH_B) and TB or marrow spacing (SP_M) over an ROI. In these methods, fuzzy skeletonization plays a crucial role in selecting sample points which are vital in determining the effectiveness of these measures.

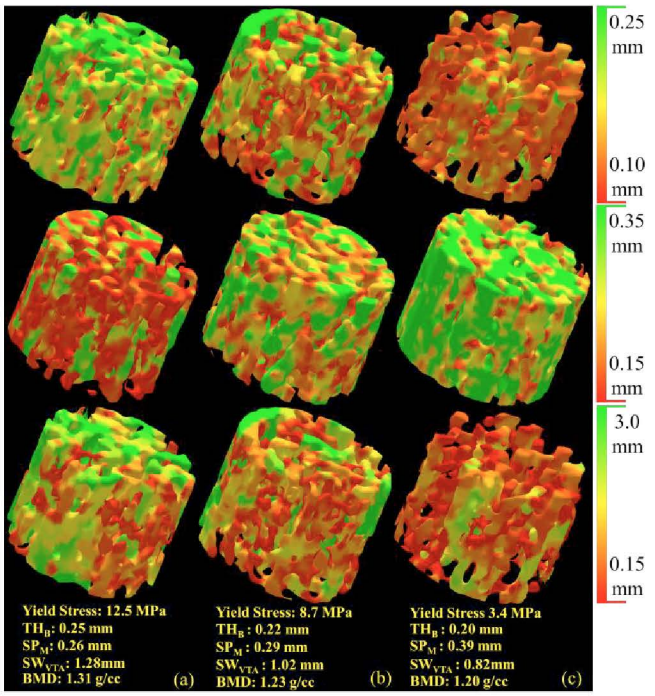

Fig. 2. Illustration of the fuzzy skeletonization based TB micro-architectural measures for three different TB specimens – (a) strong (yield stress: 12.5MPa), (b) moderate (8.7MPa) and (c) weak (3.4 Pa).

Experiments were designed to examine the ability of fuzzy skeletonization based TB micro-architectural measures to predict experimental TB strength. All experiments were performed on twelve fresh-frozen human cadaveric ankle specimens harvested from 11 body donors under the Deeded Body Program at the University of Iowa. The following sequential steps were applied on each specimen – (1) MD-CT imaging, (2) image processing, and (3) mechanical testing. All ankle specimens were kept frozen until the performance of MD-CT imaging.

High resolution MD-CT scans of distal tibia were acquired at the Iowa Comprehensive Lung Imaging center, University of Iowa on a 128 slice SOMATOM Definition Flash scanner at 120 kV, 200 effective mAs, and reconstructed at 0.2 mm slice thickness using an U70u kernel achieving high spatial resolution. Three repeat MD-CT scans of each distal tibia specimen were acquired after repositioning the specimen on the CT table before each scan.

TB MD-CT images were converted into bone mineral density (BMD) images using the INTable™ Calibration Phantom and were resampled at 150 μm isotropic voxel. These resampled BMD images were used for computation of

average BMD, TH_B, SP_M, SW_{VTA}, and SCR_{VTA} over a target ROI.

To determine TB strength, a cylindrical TB core with 8 mm in diameter and 20.9±3.3 mm in length was cored from distal tibia in situ along the proximal-distal direction. Each TB core was mechanically tested in compression using an electromechanical materials testing machine. To minimize specimen end effects, strain was measured with a 6 mm gage length extensometer attached directly to the midsection of the bone. A compressive preload of 10 N was applied and strains then set to zero. At a strain rate of 0.005 sec^{-1}, each specimen was preconditioned to a low strain with at least ten cycles and then loaded to failure. Yield stress was determined as the intersection of the stress-strain curve and a 0.2% strain offset of the modulus.

Results of TB micro-architectural measures for three specimens with different bone strengths are shown in Fig. 2. An 8% loss in BMD from the strong bone (a) to the weak bone (c) leads to a 73% loss in bone strength and manifests into 20% reduction in TB thickness, 50% increase in marrow spacing, and 36% reduction in TB surface width measure. This observation supports that TB thickness and marrow spacing are highly sensitivity to bone degeneration.

In order to examine the ability of fuzzy skeletonization based TB micro-architectural measures to predict bone strength, a linear correlation analysis between each of the four measures and the TB's experimental yield stress was performed. The image-based measures were computed over a cylindrical VOI with its axis aligned to that of distal tibia and its length and position were selected as per the data recorded during specimen preparation and mechanical testing. The results of correlation analysis between yield stress and each of the four TB measures are shown in Fig. 3. The value of R^2 of the linear correlation between bone mineral density (BMD) and TB yield stress was observed as 0.78. All four TB micro-architectural measures have demonstrated better strength to predict TB's yield stress as compared to BMD.

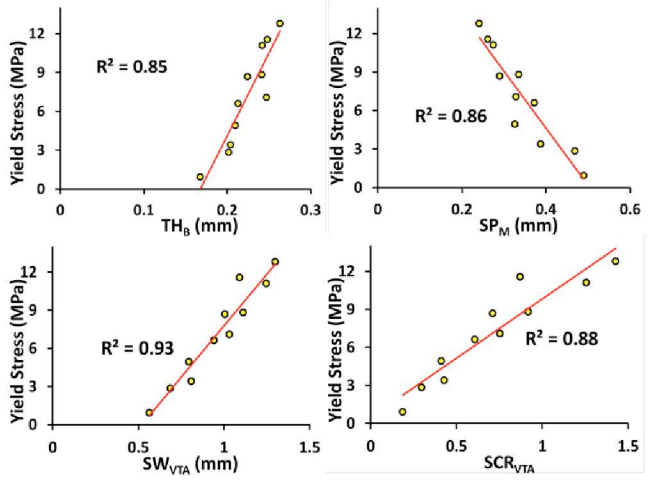

Fig. 3 Ability of different TB micro-architectural measures to predict bone strength shown in terms of R^2 values of linear correlation between yield stress and each of $\boldsymbol{TB_B}$ (a), $\boldsymbol{SP_M}$ (b), $\boldsymbol{SW_{\text{VTA}}}$ (c), and $\boldsymbol{SCR_{\text{VTA}}}$ (d).

IV. Conclusions

In this paper, we have presented a fuzzy skeletonization method and its application to quantitatively asses TB micro-architectural measures through MD-CT imaging under an *in vivo* condition. Results of a comprehensive study on twelve cadaveric ankle specimens evaluating the new method are presented. Observed results have demonstrated that fuzzy skeletonization based TB parameters are able to predict trabecular bone's experimental mechanical properties under an *in vivo* condition. Currently, we are investigating the role of the new method in characterizing different groups of human subjects with different clinical status of bone health.

Acknowledgements: This work was supported by the NIH grant R01-AR054439.

References

1. Kleerekoper, M., Villanueva, A. R., Stanciu, J., Rao, D. Sudhaker, and Parfitt, A. M.: The role of three-dimensional trabecular microstructure in the pathogenesis of vertebral compression fractures. Calcified Tissue International. 37, 594-597 (1985).
2. Wehrli, F. W., Saha, P. K., Gomberg, B. R., Song, H. K., Snyder, P. J., Benito, M., Wright, A., and Weening, R.: Role of magnetic resonance for assessing structure and function of trabecular bone. Topics in Magnetic Resonance Imaging. 13, 335-356 (2002).
3. Arcelli, C., di Baja, G. S., and Serino, L.: Distance-driven skeletonization in voxel images. IEEE Trans Pattern Anal Mach Intell. 33, 709-720 (2011).
4. Ma, C. M. and Sonka, M.: A fully parallel 3D thinning algorithm and Its applications. Computer Vision Image Understand. 64 420-433 (1996).
5. Saha, P. K., Chaudhuri, B. B., and Majumder, D. Dutta: A new shape preserving parallel thinning algorithm for 3D digital images. Pattern Recognition. 30, 1939-1955 (1997).
6. Saito, T. and Toriwaki, J.-I.: A sequential thinning algorithm for three dimensional digital pictures using the Euclidean distance transformation.In: 9th Scandinavian Conference on Image Analysis (SCIA'95), IAPR507-516 (1995).
7. Tsao, Y. F. and Fu, K. S.: A parallel thinning algorithm for 3D pictures. Computer Graphics and Image Processing. 17, 315-331 (1981).
8. Tari, Z. S. G., Shah, J., and Pien, H.: Extraction of shape skeletons from grayscale images. Computer Vision Image Understand. 66, 133-146 (1997).
9. Yim, P. J., Choyke, P. L., and Summers, R. M.: Gray-scale skeletonization of small vessels in magnetic resonance angiography. IEEE Trans Med Imaging. 19, 568-76 (2000).
10. Saha, P. K., Wehrli, F. W., and Gomberg, B. R.: Fuzzy distance transform: theory, algorithms, and applications. Computer Vision Image Understand. 86, 171-190 (2002).
11. Arcelli, C. and Di Baja, G. S.: A width-independent fast thinning algorithm. IEEE Trans Pattern Anal Mach Intell. 7, 463-74 (1985).
12. Blum, H., Ed., A transformation for extracting new descriptors of shape (Models for the Perception of Speech and Visual Form. Cambridge, MA: MIT Press, 1967.
13. Saha, P. K. and Chaudhuri, B. B.: Detection of 3-D simple points for topology preserving transformations with application to thinning. IEEE Transactions on Pattern Analysis and Machine Intelligence. 16, 1028-1032 (1994).
14. Kong, T. Y. and Rosenfeld, A.: Digital topology: introduction and survey. Computer Vision, Graphics, Image Process. 48, 357-393 (1989).
15. Saha, P. K., Xu, Y., Duan, H., Heiner, A., and Liang, G.: Volumetric topological analysis: a novel approach for trabecular bone classification on the continuum between plates and rods. IEEE Trans Med Imaging. 29, 1821-38 (2010).
16. Liu, Y. and Saha, P. K.: A new algorithm for trabecular bone thickness computation at low resolution achieved under in vivo condition.In: International Symposium on Biomedical Imaging: From Nano to Macro, San Francisco, CA (April 7-11, 2013, accepted).